



Structure sensitivity of ammonia oxidation over platinum

Ying Feng Zeng, Ronald Imbihl*

Institut für Physikalische Chemie und Elektrochemie, Leibniz-Universität Hannover, Callinstr. 3-3a, 30167 Hannover, Germany

ARTICLE INFO

Article history:

Received 25 February 2008

Revised 16 May 2008

Accepted 17 May 2008

Available online 12 November 2008

Keywords:

Platinum

Stepped platinum surface

Ammonia oxidation

Kinetics

ABSTRACT

Ammonia oxidation over different Pt single crystal orientations and a Pt foil has been studied in the 10^{-5} to 10^{-2} mbar range with rate measurements and LEED. The reaction exhibits only a moderate structure sensitivity with the activity varying in the sequence Pt foil:Pt(533):Pt(865):Pt(443):Pt(100) = 6:4:4:2:1. The activity is apparently mainly determined by the oxygen sticking coefficient which reaches 0.14 on the Pt foil. Broad hystereses in the reaction rates upon cyclic variation of the temperature are associated with reversible structural changes. The extent of reaction-induced structural changes depends strongly on the orientation, the total pressure and also on the ratio of the reactants NH_3/O_2 . On Pt(533) and Pt(443) the extent of restructuring and the hysteretic behavior was found to depend in a non-monotonic way on the total pressure. Exposure to reaction conditions at 10^{-3} mbar creates a disordered surface as seen in LEED with no LEED spots visible; but after exposure to reaction conditions at 10^{-2} mbar the integral order beams in LEED are again visible.

© 2008 Published by Elsevier Inc.

1. Introduction

The catalytic oxidation of ammonia over platinum is a key step, both in the industrial manufacturing of nitric acid and in environmental chemistry where ammonia is removed in the so-called selective catalytic reduction (SCR process) [1]. Theoretical studies as well as experimental data show that ammonia decomposition on platinum is activated through direct interaction of ammonia with chemisorbed oxygen or OH species [2–5]. Single crystal studies have been performed with Pt(100) [2,3], Pt(111) [6,7] and with stepped Pt(111) orientations [3,8–12]. Already in the very early studies of Gland et al. it was concluded that the reactivity of Pt samples in catalytic ammonia oxidation is determined by the density of steps [8]. Since two elementary steps of the reaction mechanism, dissociative oxygen chemisorption and NO decomposition are highly structure sensitive on Pt, ammonia oxidation should be structure sensitive too [13–23].

In this report we compare the activity of Pt(533), Pt(443), Pt(865), Pt(100), and a Pt foil in ammonia oxidation up into the 10^{-2} mbar range. The surfaces Pt(533) and Pt(443) are stepped (111) surfaces which differ in their step orientation as evident from the microfacet notation which is $4(111) \times 1(100)$ for Pt(533) and $7(111) \times 1(111)$ for Pt(443). Their kinetics have been studied quite in detail up to 10^{-4} mbar before [11,12]. As model system for a kinked surface we take the Pt(865) surface written $11(111) \times 2(511)$ in microfacet notation [24]. The Pt(100) surface

exhibits an adsorbate-induced surface phase transition between a catalytically active bulk-like (1×1) termination and a quasi-hexagonal reconstruction of the topmost layer (“hex”) which has a very low activity [14,25,26]. Catalytic ammonia oxidation on Pt(100) has been studied quite in detail by the group of King but mostly under unstationary reaction conditions and only below a pressure of 10^{-5} mbar [2,4].

The structure sensitivity of ammonia oxidation contains a dynamic aspect which is that the substrate structure is modified by the reaction. With varying extent this is certainly true for all catalytic reactions but the effect is particularly strong for ammonia oxidation on Pt where a visible roughening of Pt/Rh gauzes used in the Ostwald process already occurs during the first minutes of operation. Phenomenological studies focusing on reaction-induced morphological changes have been conducted with small Pt spheres at high pressure [27,28]. With LEED and STM restructuring was studied in the 10^{-5} and 10^{-4} mbar range on Pt(533) and Pt(443) [3,11,29]. On Pt(533) a reversible doubling of the step height occurs associated with a change in the selectivity of the reaction. The reversible restructuring of Pt(533) shows up in a hysteresis of the N_2 and NO production rates upon cycling the temperature. On Pt(443) already at 300 K the initially straight step edges start to meander upon ammonia adsorption [3].

The questions are to which extent the different orientations undergo restructuring and how the restructuring depends on the total pressure. Furthermore, the restructuring should be associated with an activation or deactivation of the catalyst and with selectivity changes. In this study we address these questions using rate measurements and LEED to follow reaction-induced restructuring as we increase the pressure from 10^{-5} mbar to 10^{-2} mbar. In this

* Corresponding author.

E-mail address: gatzen@pci.uni-hannover.de (R. Imbihl).

way we only partially bridge the pressure gap between UHV and the conditions of the Ostwald process but already in this range we find quite unexpected results. The ordering we observe after restructuring seems to depend in a non-monotonic way on the total pressure.

2. Experimental

The reaction was studied in a standard UHV system equipped with LEED, a retarding field analyzer for Auger electron spectroscopy and a differentially pumped quadrupole mass spectrometer (QMS) for rate measurement. The base pressure in the UHV system was 2×10^{-10} mbar. The sample was heated indirectly by a filament behind the backside of the crystal via either radiation or electron bombardment. Samples were prepared by repeated cycles of Ar-ion sputtering, heating in oxygen ($P_{\text{oxygen}} = 5 \times 10^{-6}$ mbar), followed by annealing to 1300 K. The sample temperature was measured with a thermal couple spot-welded to the side of the sample. A PID controller was used for temperature programmed reaction (TPR) experiments. The gas purity was 5.0 for oxygen and 2.5 for ammonia. The Pt(533) and Pt(443) samples were the same as used in previous experiments [3,11,29].

In order to investigate this reaction in an intermediate pressure range between 10^{-3} and 1 mbar, a high pressure reaction cell was connected to the UHV main chamber via a sample transfer system. After cleaning, the sample is transferred into the reaction cell. During rate measurements in the low pressure regime a cone with 2 mm orifice, which separates the differentially pumped QMS from the main chamber, was brought 1 mm in front of the sample surface. In this way only species originating from the sample surface are detected. For rate measurements in the high pressure cell a stainless steel tube with a 2 mm orifice was brought approximately 1 mm in front of the sample surface.

For calibration the gases NH_3 , O_2 , N_2 , and NO were introduced into the main chamber so that the QMS signal could be related to the real pressure. From the measured pressure increase under reaction conditions the number of particles desorbing from the sample surface was calculated with ideal gas equation using the known pumping rate and the surface area of the sample.

3. Results

3.1. Structure sensitivity

In Fig. 1 we compare the activity of two stepped Pt (111) surfaces, Pt(533) and Pt(443), with that of a kinked surface, Pt(865), with a Pt(100) sample, and with a Pt foil. The samples were subjected to heating/cooling cycles in an NH_3/O_2 atmosphere with a 1:1 ratio of the partial pressures at a total pressure of 1×10^{-5} mbar. The same y-scaling has been used for all samples so that the rate curves can be compared directly. Structural models of the single crystal orientations are displayed in Fig. 2. The relatively small hystereses we observe on Pt(443), Pt(865), and on Pt(533) can be attributed mainly to transients caused by a heating/cooling rate of 0.5 K/s which is still too large to ensure true steady state conditions. The larger hystereses we see on Pt(100), and the Pt foil are clearly true hystereses caused by reversible structural changes of the Pt substrate. A broad hysteresis connected to reaction-induced structural changes has also been observed with Pt(533) but only at a total pressure substantially beyond 1×10^{-5} mbar [11,29]. At the 1×10^{-5} mbar employed here we therefore do not see such a broad hysteresis.

Qualitatively the rate curves of all samples are similar. N_2 formation is the dominant reaction pathway at low temperature whereas at high temperature NO production prevails. If we take the maximum in N_2 production as a measure of the catalytic activity we obtain the following sequence in catalytic activity: Pt

foil:Pt(533):Pt(865):Pt(443):Pt(100) = 6:4:4:2:1. We also note that with exception of Pt(100) the N_2 rate maxima shift to lower temperature with increasing catalytic activity of the sample.

A hysteresis in the activity can arise (i) due to reversible structural changes or an activation/deactivation by oxide formation and reduction (ii) due to the inhibitory effect of adsorbates on the adsorption of reactants or (iii) through the formation and removal of surface contaminants. Realistic mathematical models of ammonia oxidation on Pt did not reveal any kinetic multistability which makes (ii) rather unlikely [5,9]. *In situ* XPS measurements of Pt(533)/ $\text{NH}_3 + \text{O}_2$ showed that up to 1 mbar no Pt oxide forms [30]. Reversible restructuring and a potential influence of surface contaminants remain therefore as possible causes for the hystereses. For Pt(100) the hysteresis in the reaction rates is clearly associated with the $(1 \times 1) \leftrightarrow \text{hex}$ phase transition. The low rate branch is connected with inactive hex reconstructed surface whereas the high rate branch belongs to the active (1×1) termination of the substrate [2,31].

As will be shown below LEED data taken after completion of the measurements reveal a very drastic restructuring of the Pt(865) surface. This indicates that structural changes take place in the heating/cooling cycles. For the Pt foil we have no means of detecting structural changes but the texture of the foil contains grains with (100) and (111) orientations which have been shown to undergo restructuring, i.e. via the adsorbate-induced surface phase transition in the case of Pt(100) and via reaction-induced faceting in the case of Pt(111) [26,28]. We can therefore assume that the large hysteresis we observe with the Pt foil presumably has the same origin.

For characterizing the surface *in situ* we can measure the reactive sticking coefficient of oxygen. Due to the geometric arrangement of the QMS which is shielded behind a cone, only molecules reflected from the surface can enter the cone to be detected. We obtain the reactive sticking coefficient s_{reac} following the variation of the partial pressures of the reactants, i.e. of O_2 or NH_3 . Denoting the signal of a gas without reaction by I_0 and during reaction with I we calculate the reactive sticking coefficient

$$s_{\text{reac}} = \frac{I_0 - I}{I_0}.$$

In this case the reaction rate at 300 K was assumed to be negligible so that the partial pressures at 300 K should represent I_0 .

The variation of the reactive sticking coefficient (s_{reac}) of oxygen during the temperature cycling experiments is reproduced in Fig. 3 for the Pt foil, Pt(100) and Pt(865). The variation of s_{reac} reflects in general rather well the behavior of the reaction rates during the T -cycling experiments displayed in Fig. 1. For Pt(100), for example, the low reactivity of the cooling branch is due to the low oxygen sticking coefficient on the hex phase which according to the literature is as low 10^{-3} for a structurally nearly perfect hex phase [2,14]. During heating up s_{reac} does not reach the value of 0.2 reported for oxygen sticking on the bare Pt(100)- (1×1) surface but only goes up to 0.03 [2]. The discrepancy might indicate that the hex phase has not been lifted completely during cooling down so that a significant portion of the surface remains in the inactive hex state all the time.

In contrast to Pt(100) the activity of the Pt foil increases by heating up as evidenced by a higher rate maxima for N_2 and NO and a higher s_{reac} in Figs. 1 and 3, respectively. Remarkably, between roughly 600 and 800 K the selectivity changes drastically from preferential N_2 formation on heating up to NO as main product during cooling down. The increase in the overall activity after heating is reflected by the increase in s_{reac} in Fig. 3. The comparison of the Pt foil with Pt(865) shows that on these two samples s_{reac} reaches about 0.14 and 0.12, respectively.

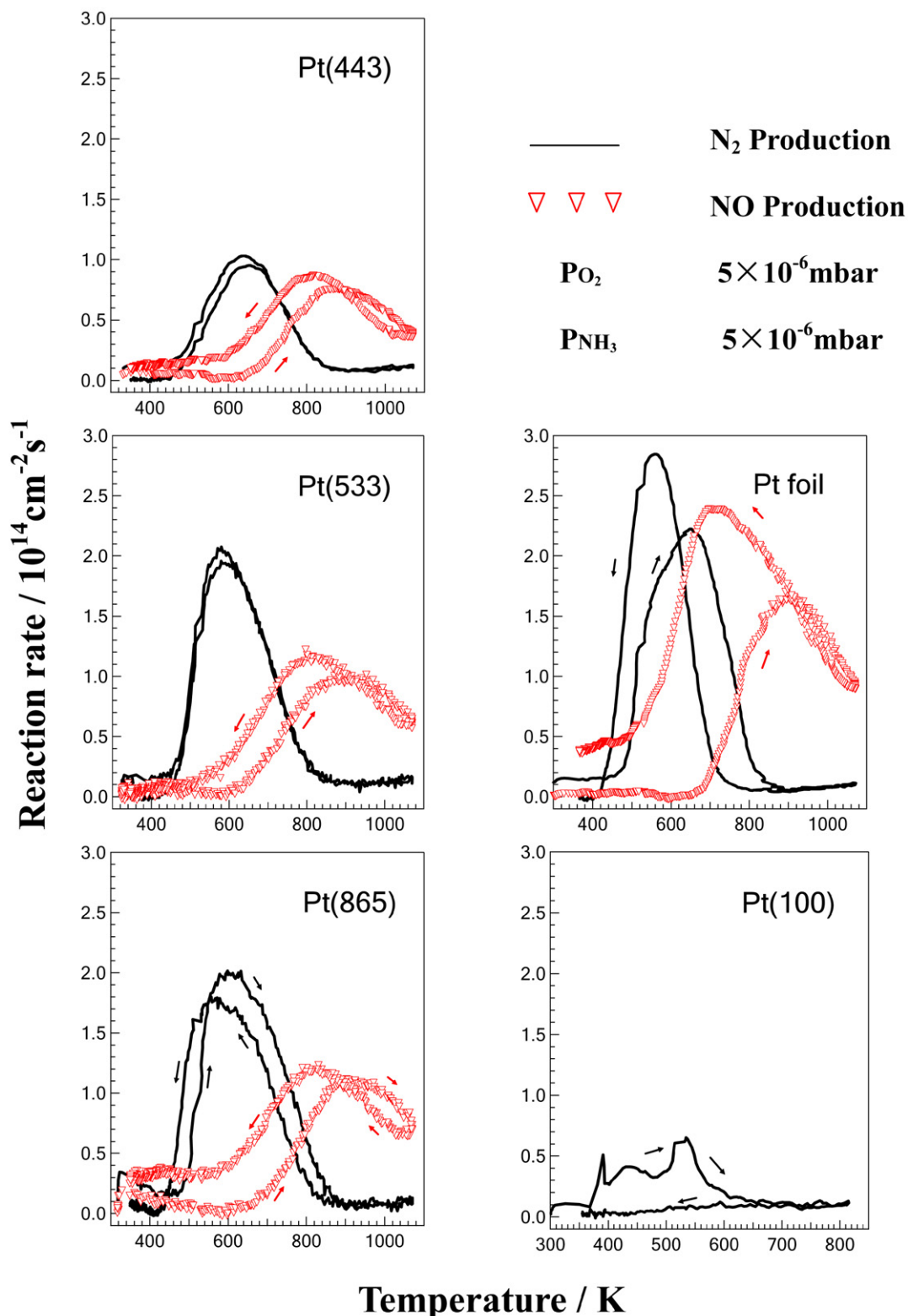


Fig. 1. Comparison of the catalytic activity of Pt(533), Pt(443), Pt(865), Pt(100), and of a Pt foil in the 10^{-5} mbar range with a 1:1 mixing ratio of the gases. The ramping speed in the T -cycling experiments was 30 K/min. Due to the relatively high ramping rate the hystereses with exception of Pt(100) are mainly caused by transients.

3.2. Influence of total pressure

We studied the influence of the total pressure on the kinetics of N_2 and NO production in the 10^{-5} – 10^{-2} mbar range. Figs. 4 and 5 display the results for Pt(533) and Pt(443) obtained for a 1:1 ratio NH_3/O_2 of the reactants and with identical ramping

speed. In all experiments we started with a freshly prepared surface after Ar-ion sputtering, oxygen treatment and annealing to 1100 K. Experiments with a pressure at or above 10^{-3} mbar were carried out in the high pressure chamber, and with a pressure below 10^{-3} mbar in the main chamber. Fig. 6 displays for Pt(533), Pt(443), and Pt(865) a plot of the maximum N_2 production rate

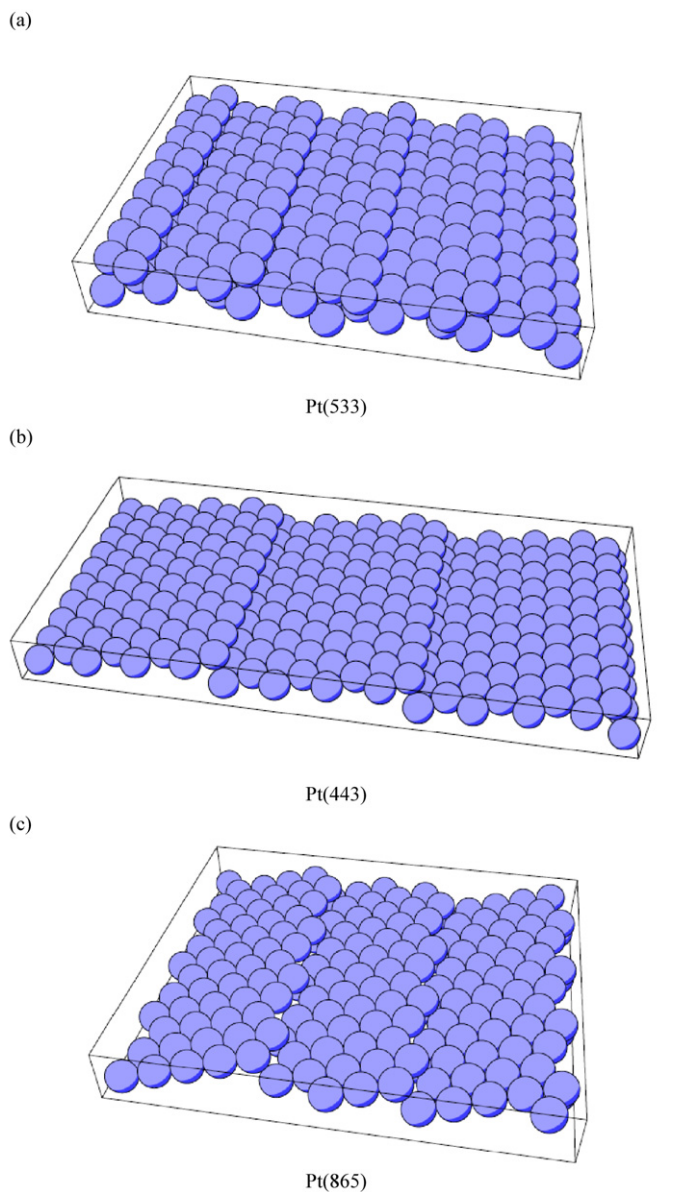


Fig. 2. Structural models of different Pt single crystal surfaces: (a) Pt(533), (b) Pt(443), and (c) Pt(865).

versus the total pressure. Up to 10^{-3} mbar the N_2 production scales with the total pressure but beyond 10^{-3} mbar the rate slows down. At 10^{-2} mbar the measured rate is lower by roughly a factor of three compared to the rate that scaling with total pressure would predict. According to experiments conducted with He mixing mass transport limitations start to play a role only beyond 10 mbar at catalyst temperatures above 660 K [5]. More likely is that at 10^{-2} mbar the adsorbate coverages become large enough to slow down considerably the adsorption kinetics so that scaling of the rate with the total pressure can longer be expected.

As shown in Fig. 4, at a total pressure of 6×10^{-5} mbar Pt(533) displays a broad hysteresis in the N_2 and NO production which was shown to be due to a reversible doubling of the step height upon heating [11,29]. At 6×10^{-5} mbar the double-atomic steps were demonstrated to be present roughly between 600 K and 800 K on the heating branch. Increasing the total pressure to 1×10^{-3} mbar considerably enhances the N_2 hysteresis while the NO hysteresis practically disappears. The latter is probably a consequence of shifting the NO rate maximum to a higher temperature outside the

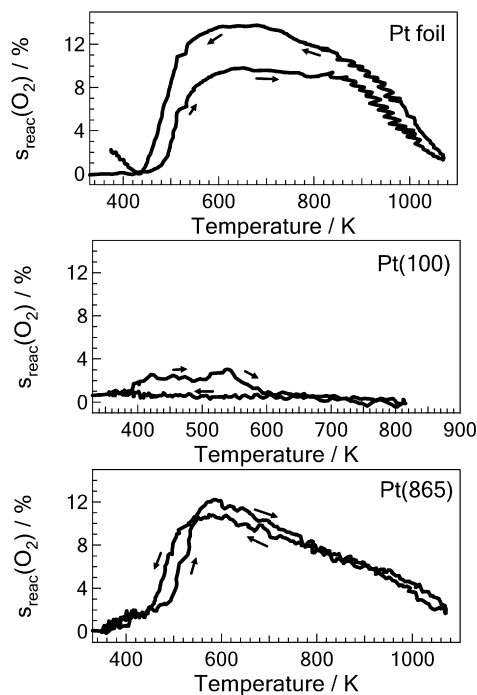


Fig. 3. Variation of reactive oxygen sticking coefficient (s_{reac}) during temperature cycling experiments with a Pt foil, Pt(865) and Pt(100). The total pressure is in the 10^{-5} mbar range, and a 1:1 mixing ratio of the gases NH_3 and O_2 is used. The ramping speed in the T -cycling experiments was 30 K/min.

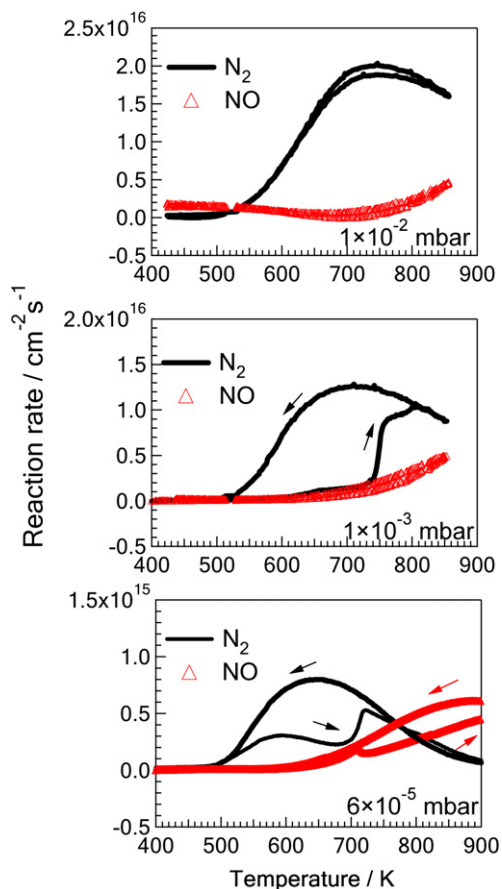


Fig. 4. Effect of the total pressure on the kinetics of N_2 and NO production on Pt(533), the experiments are conducted in the 10^{-5} – 10^{-2} mbar range under a feed composition 1:1 and with a ramping speed of 0.5 K/s.

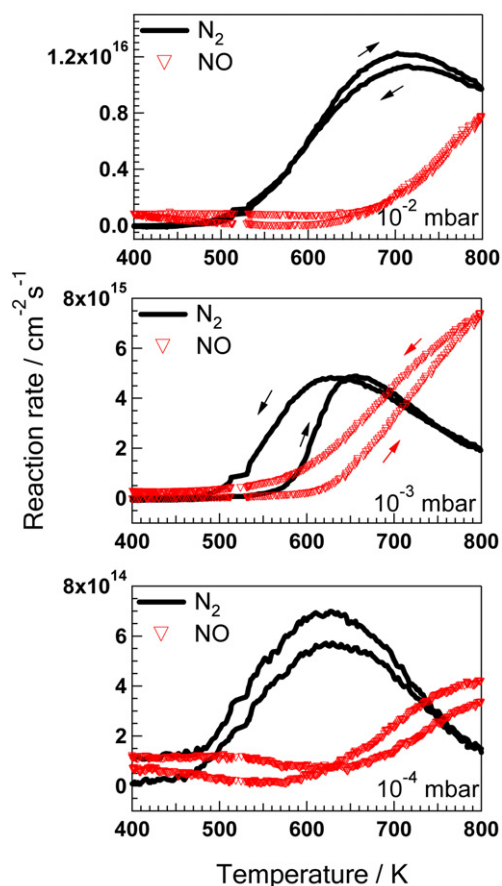


Fig. 5. Effect of the total pressure on the kinetics of N_2 and NO production on Pt(443), the experiments are conducted in the 10^{-5} – 10^{-2} mbar range under a feed composition 1:1 and with a ramping speed of 0.5 K/s.

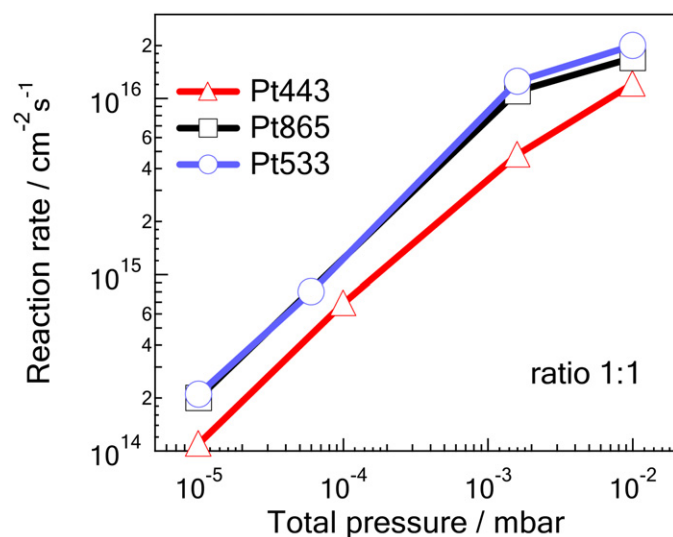


Fig. 6. Dependence of the maximum rate of N_2 production on the total pressure. The Pt orientations Pt(533), Pt(443), and Pt(865) are compared. The same reaction conditions are applied with a mixing ratio of ammonia to oxygen of 1:1.

T -cycling window. Quite surprisingly, a further increase of the total pressure to 1×10^{-2} mbar leads to a vanishing hysteresis.

On Pt(443) practically no hysteresis is seen at 10^{-5} mbar and at 10^{-4} mbar but increasing the total pressure to 1×10^{-3} mbar causes the appearance of a substantial hysteresis as evidenced by Fig. 5. After a further rise to 1×10^{-2} mbar the hysteresis vanishes

again similar to the behavior of Pt(533). The hystereses of Pt(533) and Pt(433) are all counterclockwise, i.e. heating up leads to an activation of the catalyst.

The preceding measurements show an unexpected result: a non-monotonic variation of the hysteretic behavior with pressure for both orientations, Pt(533) and Pt(443). At low pressure ($p < 10^{-5}$ mbar) no hysteresis occurs, at intermediate pressure a very pronounced hysteresis is observed and at high pressure (10^{-2} mbar) the hysteresis vanishes again. The two orientations Pt(533) and Pt(443) differ in so far as Pt(533) displays a pronounced hystereses at 10^{-5} and 10^{-4} mbar whereas no hysteresis exist for Pt(443) in this pressure range. The explanation as verified by LEED and STM is that on Pt(533) a reversible doubling of the step height occurs while the average step separation remains constant on Pt(443).

With increasing total pressure in general the risk of a surface contamination rises for two reasons. The partial pressure of contaminants in the gas phase increases and the higher chemical potential of the reactants enhances the segregation of bulk contaminants to the surface. One might suspect that contamination effects are responsible for the pressure dependent vanishing of the hystereses but so far Auger electron spectroscopy provided no indication of surface contaminants. Moreover, the segregation of Si which leads to SiO_2 formation on the Pt surface would cause an irreversible reduction of catalytic activity which is not what we see. On the other hand, since we cannot completely rule out a potential influence of contaminants this possibility should still be taken into account. In the following we try to establish a connection between the rate hystereses and changes in the catalytic properties of Pt(533) and Pt(443).

For Pt(533) it was demonstrated that the doubling of the step height under reaction conditions is associated with a change in the selectivity from N_2 towards NO formation. Since the availability of oxygen controls the selectivity towards NO an increase in the oxygen sticking coefficient could explain the observed change in selectivity. The data in Fig. 7a recorded in the 10^{-4} mbar range show that upon heating s_{reac} increases sharply at 700 K which is roughly the temperature where we expect the doubling of the step height to occur. s_{reac} , however, also remains high during cooling down but during cooling down the steps remains single-atomic as shown in earlier measurements [11,29]. Evidently s_{reac} cannot be determined by the step structure alone but apparently also the adsorbate coverages determine s_{reac} by blocking sites for adsorption. In addition, also local structural changes which do not show up in LEED might play a role. Measurements of s_{reac} with different ratios $NH_3:O_2$ show that the hysteresis becomes smaller the more oxygen is in excess. For a 10 fold excess of O_2 the hysteresis practically vanishes.

With LEED the surface structure of Pt(533), Pt(443), and Pt(865) was examined after exposure to reaction conditions. The beam profiles of the split (1, 0)-beam after the hysteresis measurements in the 10^{-2} mbar range are displayed in Fig. 8. On all three surfaces the beam intensity strongly decreased in comparison to their initial values. On Pt(865) the ordering after the reaction is so poor that the LEED spots are hardly discernible from the background. The splitting of the spot is no longer visible and instead a very small peak appears at the middle position of the original spot splitting. On Pt(533) we observe a widening of the spot splitting by roughly 20%. On Pt(433) the spot splitting remained unchanged but the FWHM of the spots increased and the maximum intensity dropped by 50%. This indicates some disordering caused by the reaction. Apparently the average terrace width on Pt(443) has not been changed by the reaction in contrast to Pt(533) where the average terrace width decreased by around 20%.

An overview summarizing the observations with LEED and the hysteresis measurements of the different orientations in the differ-

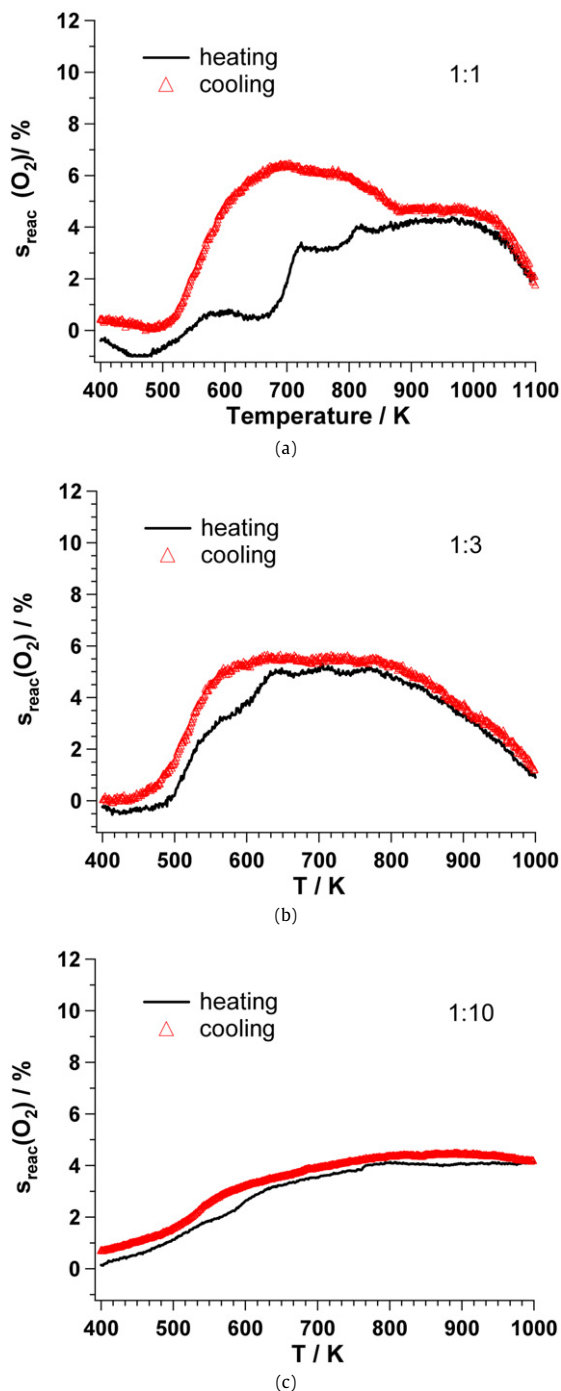


Fig. 7. Reactive sticking coefficient of oxygen during ammonia oxidation on Pt(533) under varying feed composition $\text{NH}_3:\text{O}_2$, from 1:1 to 1:10. The ramping speed is 10 K/min. The total pressure is at around 10^{-4} mbar.

ent pressure ranges is given in Table 1. We first focus on Pt(533) and Pt(443). The LEED data as well as the hysteresis measurements do not exhibit a monotonic variation with pressure. Both orientations, Pt(533) and Pt(443) become disordered at 10^{-3} mbar but at higher pressure, at 10^{-2} mbar, some ordering is present again. Similarly, both orientations display broad hystereses at 10^{-3} mbar but at 10^{-2} mbar the hystereses vanish for both orientations. In order to exclude a contamination effect, we changed the sequence in which the experiments were performed. First ammonia oxidation was carried out at 10^{-2} mbar, subsequently the total pressure was reduced to 10^{-3} mbar. Also in this sequence we find a hysteresis at 10^{-3} mbar but not at 10^{-2} mbar.

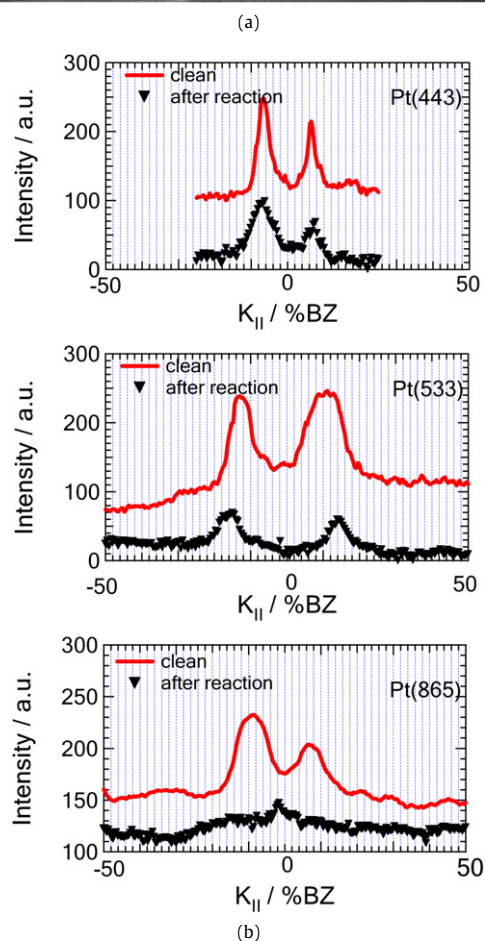
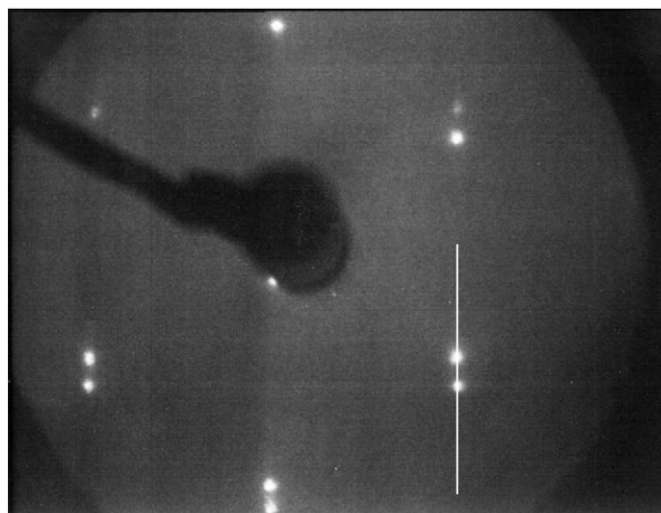


Fig. 8. (a) A LEED pattern of Pt(533) showing the profile window along which the intensity profiles reproduced in (b) were taken. (b) LEED spot profiles showing reaction-induced restructuring in the 10^{-2} mbar range. Beam intensity profiles of the (1,0)-beam are taken between the (1, -1/2) and the (1, 1/2) beam which is the direction of the spot-splitting. The sample was exposed to NH_3/O_2 at 10^{-2} mbar during temperature cycling from 300 to 800 K for 150 min. The mixing ratio is 1:1, LEED beam energy $E = 110$ eV.

On Pt(865) the behavior of Pt(865) is insofar different from that of Pt(533) and Pt(443) as a hysteresis is only visible at low pressure, at 10^{-4} mbar, where the surface is also still well ordered. At higher pressure the surface undergoes complete restructuring and the hysteresis disappears. The most stable surface of all orientations we investigated is Pt(100) as evidenced by Table 1. Up to

Table 1Overview of the LEED and *T*-cycling experiments over different pressure ranges for Pt(533), Pt(443), Pt(865), and Pt(100).

Pressure range	Pt(533)		Pt(443)		Pt(865)		Pt(100)	
	Hysteresis in reaction rate	Surface ordering/LEED	Hysteresis in reaction rate	Surface ordering/LEED	Hysteresis in reaction rate	Surface ordering/LEED	Hysteresis in reaction rate	Surface ordering/LEED
10 ⁻⁴ mbar	Yes	Ordered (1 × 1)	No	Ordered (1 × 1)	Yes	Ordered (1 × 1)	Yes	Ordered (1 × 1)
10 ⁻³ mbar	Yes	Disordered	Yes	Disordered	No	Disorder	Yes	Ordered (1 × 1)
10 ⁻² mbar	No	Ordered (1 × 1)	No	Ordered (1 × 1)	No	^a	Yes	Ordered (1 × 1)

^a Diffuse broad spot with low intensity.

10⁻² mbar this surface remains well-ordered independent of the pressure range.

4. Discussion

Using the maximum in N₂ production as a measure for catalytic activity the activity ratio Pt foil:Pt(533):Pt(865):Pt(443):Pt(100) = 6:4:4:2:1 was obtained. The choice of the maximum in N₂ production as a measure for catalytic activity contains some arbitrariness because the height of the maximum will also depend on the temperature where the branching to preferential NO formation takes place. If we use instead the maximum in the reactive oxygen sticking coefficient, *s*_{reac}, we come to a corresponding activity ratio of 4.5:2:4:2:1. With exception of Pt(533) the picture is very similar to the ratio obtained with the maximum in N₂ production.

In this study of different orientations the Pt(111) surface has not been included but since the oxygen sticking coefficient of a structurally perfect Pt(111) surface is very low [32], it is probably safe to assume that their catalytic activity is very low too. The higher activity of Pt(533) in the N₂ production rate as compared to Pt(443) which amounts to a factor of two (Fig. 1) can be attributed to the higher step density of Pt(533) which is higher by a factor of 7/4. What also might play a role could be dependence of the activity on the step orientation. With regard to Pt(100)-(1 × 1) one might suspect a higher activity of (100) steps as compared to steps with (111) orientation but this remains to be shown. Comparing Pt(865) with the stepped orientations in Fig. 1, one can conclude from their similar activity that the additional presence of kinks does not have a dramatic effect on the activity.

Quantum chemical studies of ammonia activation by O_{ad} and OH_{ad} on flat and stepped Pt(111) surfaces indicated a small influence of the surface structure on the Pt activity as far as the pure decomposition steps of NH_x (*x* = 1–3) are concerned [3]. The main factors causing a structure sensitivity of ammonia oxidation on Pt are the adsorption of oxygen and ammonia and NO formation/decomposition. Ammonia adsorption on Pt surfaces exhibits only a moderate structure sensitivity [33], but oxygen sticking on Pt is known to vary over three orders of magnitude depending on the structure from about 10⁻³ on Pt(100)-hex to a value close to one on Pt(210) [2,15,22]. Detailed studies of oxygen adsorption on Pt(533) have been performed in the group of Hayden [17]. The different studies all agree that oxygen adsorption on Pt is largely determined by structural defects, i.e. by atomic steps and kinks [34].

The data shown here indicate that kinked surface have a low structural stability under reaction conditions followed by stepped surfaces. The Pt(100) surface exhibits the highest stability of all studied surfaces under reaction conditions. This is consistent with the results of Schmidt et al. who studied small single crystal spheres of Pt in a NH₃/O₂ atmosphere and found that after exposure to reaction conditions in the mbar range (100) orientations survive [27,28].

Previous LEED and STM investigations of Pt(533)/NH₃ + O₂ conducted in the 10⁻⁵ and 10⁻⁴ mbar range have shown that the rate hysteresis is connected with reversible structural changes, i.e. a reversible doubling of the step height [29]. In the pressure range investigated here no in situ methods were available to mon-

itor structural changes during the rate hystereses. The fact that at 10⁻³ mbar large hystereses on Pt(533) and Pt(443) are connected with a disordered surface (see Table 1) seems to be in contradiction to the previous statement relating rate hystereses with reversible structural changes. However, the LEED data in Table 1 only show the state of the surface after completion of the experiment. This leaves the possibility that during the *T*-cycles an ordered surface may exist in a certain parameter range. A second possibility is that LEED only shows the absence of long range order while some short range order may still exist. Local restructuring without long range order might therefore be responsible for the rate hystereses found on disordered surfaces.

One rather unexpected phenomenon was the non-monotonic variation of the hysteretic behavior and of the surface ordering with total pressure observed with Pt(533) and Pt(443) (Table 1). In principle, one could envision a surface which is roughened by the reaction at some intermediate pressure but which orders again as the dynamics of the reaction beyond a certain threshold become large enough to overcome kinetic barriers preventing ordering. At the present stage, this is pure speculation and experiments extending beyond 10⁻² mbar are required in order to substantiate this interesting possibility.

5. Conclusions

The results obtained with different Pt orientations studied in the 10⁻⁵ to 10⁻² mbar show that ammonia oxidation on platinum is only a moderately structure sensitive reaction. The different reactivity is essentially determined by the difference in the oxygen sticking coefficient. The catalytic activity is highest on the Pt foil and then decreases in the order Pt(865), Pt(533), Pt(443) and Pt(100). The extent of reaction-induced restructuring depends strongly on the total pressure, the orientation and the mixing ratio of reactants. On Pt(533) and Pt(443) we observe a non-monotonic dependence of the amount of restructuring on the total pressure: increasing restructuring with pressure leads to a completely disordered surface in LEED at 10⁻³ mbar but at even higher pressure, at 10⁻² mbar, the ordering of the surfaces is partially restored.

Acknowledgments

Assistance from Dr. Sebastian Günter in the experiments is gratefully acknowledged. The authors are indebted to the group of M. Baerns for supplying a Pt foil as sample. This work was supported by the DFG under the priority program 1091 'Bridging the gap between ideal and real systems in heterogeneous catalysis'.

References

- [1] T.H. Chilton, in: The Manufacture of Nitric Acid by the Oxidation of Ammonia, in: Chemical Engineering Progress Monograph Series, vol. 3, Am. Inst. Chem. Eng., New York, 1960.
- [2] J.M. Bradley, A. Hopkinson, D.A. King, J. Phys. Chem. 99 (1995) 17032.
- [3] R. Imbihl, A. Scheibe, Y.F. Zeng, S. Gunther, R. Kraehnert, V.A. Kondratenko, M. Baerns, W.K. Offermans, A.P.J. Jansen, R.A. Van Santen, Phys. Chem. Chem. Phys. 9 (2007) 3522.

- [4] M. Kim, D.A. King, S.J. Pratt, *J. Am. Chem. Soc.* 122 (2000) 2409.
- [5] W.K. Offermans, A.P.J. Jansen, R.A.v. Santen, *Surf. Sci.* 600 (2006) 1714.
- [6] M. Asscher, W.L. Guthrie, T.-H. Lin, G.A. Somorjai, *J. Phys. Chem.* 88 (1984) 3233.
- [7] W.D. Mieher, W. Ho, *Surf. Sci.* 322 (1995) 151.
- [8] J.L. Gland, V.N. Korchak, *J. Catal.* 53 (1978) 9.
- [9] W.L. Guthrie, J.D. Sokol, G.A. Somorjai, *Surf. Sci.* 109 (1981) 390.
- [10] D.G. Löffler, L.D. Schmidt, *Surf. Sci.* 59 (1976) 195.
- [11] A. Scheibe, U. Lins, R. Imbihl, *Surf. Sci.* 577 (2005) 1.
- [12] A. Scheibe, M. Hinz, R. Imbihl, *Surf. Sci.* 576 (2005) 131.
- [13] H. Wang, R.G. Tobin, D.K. Lambert, A.L. DiMaggio, G.B. Fisher, *Surf. Sci.* 372 (1997) 267.
- [14] K. Griffiths, T.E. Jackman, J.A. Davies, P.R. Norton, *Surf. Sci.* 138 (1984) 113.
- [15] N. Freyer, M. Kiskinova, G. Pirug, H.P. Bonzel, *Surf. Sci.* 166 (1986) 206.
- [16] A. Rar, T. Matsushima, *Surf. Sci.* (1994) 89.
- [17] A.T. Gee, B.E. Hayden, *J. Chem. Phys.* 113 (2000) 10333.
- [18] V.I. Savchenko, N.I. Efremova, *React. Kinet. Catal. Lett.* 56 (1995) 97.
- [19] J.M. Gohndrone, R.I. Masel, *Surf. Sci.* 209 (1989) 44.
- [20] J.M. Gohndrone, Y.O. Park, R.I. Masel, *J. Catal.* 95 (1985) 244.
- [21] M. Sander, R. Imbihl, G. Ertl, *J. Chem. Phys.* 97 (1992) 5193.
- [22] R.J. Gorte, L.D. Schmidt, J.L. Gland, *Surf. Sci.* 109 (1981) 367.
- [23] T. Sugisawa, J. Shiraiishi, D. Machihara, K. Irokawa, H. Miki, C. Kodama, T. Kuriyama, T. Kubo, H. Nozoye, *Appl. Surf. Sci.* 169–170 (2001) 292.
- [24] M.A.V. Hove, G.A. Somorjai, *Surf. Sci.* 92 (1980) 489.
- [25] P.A. Thiel, R.J. Behm, P.R. Norton, G. Ertl, *J. Chem. Phys.* 78 (1983) 7448.
- [26] X.-C. Guo, J.M. Bradley, A. Hopkinson, D.A. King, *Surf. Sci.* 310 (1994) 163.
- [27] R.W. McCabe, T. Pignet, L.D. Schmidt, *J. Catal.* 32 (1974) 114.
- [28] M. Flytzani-Stephanopoulos, L.D. Schmidt, *Prog. Surf. Sci.* 9 (1979) 83.
- [29] A. Scheibe, S. Günther, R. Imbihl, *Catal. Lett.* 86 (2003) 33.
- [30] S. Günther, A. Scheibe, H. Bluhm, M. Haevecker, E. Kleimenov, R. Schlögl, A. Knop-Gericke, R. Imbihl, *J. Phys. Chem. C* 112 (2008) 15382.
- [31] M. Rafti, F. Lovis, Y. Zeng, R. Imbihl, *Chem. Phys. Lett.* 446 (2007) 323.
- [32] C.T. Campbell, G. Ertl, H. Kuipers, J. Segner, *Surf. Sci.* 107 (1981) 220.
- [33] J.M. Gohndrone, C.W. Olsen, A.L. Backman, T.R. Gow, E. Yagasaki, R.I. Masel, *J. Vac. Sci. Technol. A* 7 (1989) 1986.
- [34] L. Vattuone, L. Savioia, M. Rocca, *Surf. Sci. Rep.* 63 (2008) 101.